Taylor & Francis
Taylor & Francis Group

## CONGENITAL HEART DISEASE

# Magnetic Resonance Imaging Evaluation of Congenital Heart Disease: Conotruncal Anomalies

**Adam L. Dorfman, MD and Tal Geva, MD**

*Department of Cardiology, Children's Hospital Boston, Boston, Massachusetts, USA;*
*Department of Pediatrics, Harvard Medical School, Boston, Massachusetts, USA*

## ABSTRACT

Conotruncal anomalies comprise a diverse group of congenital heart defects involving the outflow tracts of the heart and the great vessels, including tetralogy of Fallot, transposition of the great arteries, truncus arteriosus, interrupted aortic arch, and other anomalies. Cardiovascular magnetic resonance (CMR) imaging plays an increasingly important role in the evaluation of patients with these lesions. Advances in CMR allow comprehensive assessment of cardiovascular anatomy, ventricular function, flow, and myocardial perfusion and viability. This article reviews the clinical aspects and the application of CMR before and after surgery in key conotruncal anomalies.

## INTRODUCTION

Conotruncal anomalies refer to a group of congenital heart defects involving the outflow tracts of the heart and the great vessels. Examples include tetralogy of Fallot, transposition of the great arteries, double-outlet ventricle, truncus arteriosus, type B interrupted aortic arch, conal septal defect (also known as subpulmonary ventricular septal defect [VSD]), aorto-pulmonary window, and anatomically corrected malposition of the great arteries. Developmental abnormalities of the embryonic conus arteriosus (infundibulum) and the truncus arteriosus may result in abnormal ventriculo-arterial alignments and connections, outlet septation defects, or outlet hypoplasia, stenosis, or atresia. The outflow tract of the embryonic univentricular heart begins with a common outlet that undergoes a complex, highly choreographed sequence of events that results in complete separation of the left and right ventricular outflow tracts, which

lead into the aorta and main pulmonary artery. Numerous genes tightly control this process and migration of mesenchymal cells from the embryonic neural crest is critical to the development of these areas. Genetic errors and faulty migration of neural crest cells are likely responsible for many of the defects discussed below.

Cardiovascular magnetic resonance imaging (CMR) plays an important role in the evaluation of patients with these lesions. CMR overcomes many of the limitations of echocardiography (e.g., restricted acoustic windows), computed tomography (e.g., exposure to ionizing radiation, lack of functional information), and cardiac catheterization (e.g., ionizing radiation exposure, morbidity, and high cost). This review discusses the clinical aspects of several conotruncal anomalies and their evaluation by CMR.

## TETRALOGY OF FALLOT

Tetralogy of Fallot (TOF) is the most common type of cyanotic CHD with an incidence of 356 per million live births (1). Although TOF involves several anatomic components, the anomaly is thought to result from a single developmental anomaly—underdevelopment of the subpulmonary infundibulum (conus) (2, 3). The anatomy is characterized by infundibular and valvar pulmonary stenosis associated with anterior, superior, and leftward deviation of the infundibular (conal) septum, hypoplasia of the pulmonary valve annulus and thickened leaflets. The degree of right ventricular outflow tract (RVOT) obstruction varies from mild to complete obstruction (i.e., TOF with pulmonary

atresia). The size of the mediastinal pulmonary arteries varies considerably. Although in some patients they can be dilated (e.g., TOF with absent pulmonary valve syndrome), more commonly their diameter ranges from normal to hypoplastic. In some patients, the pulmonary arteries are discontinuous or absent. In patients with pulmonary atresia or diminutive or absent branch pulmonary arteries, pulmonary blood flow may come from a patent ductus arteriosus, from collateral vessels arising from the aorta or its branches, or from both sources. The VSD in TOF is usually located between the malaligned conal septum superiorly and the muscular septum inferiorly (termed *conoventricular septal defect* [4]). The VSD is usually large, but it can rarely be restrictive (5). The aortic valve is rotated clockwise (as viewed from the apex) and is positioned above the ventricular septal crest, committing to both the LV and to the RV. In 5–6% of patients with TOF, a major coronary artery crosses the RVOT (6). Most commonly, the left anterior descending coronary artery originates from the right coronary artery and traverses the infundibular free wall before reaching the anterior interventricular groove. Preoperative identification of a major coronary artery crossing the RVOT is important to avoid inadvertent damage to the coronary artery during surgery.

The etiology of TOF is unknown, but recent data suggests that genetic abnormalities may play an important role, especially chromosome 22q11 deletion and other genetic defects (7–14). Additional cardiovascular and non-cardiac anomalies can be associated with TOF (15). Although the clinical presentation and course of patients with TOF vary, most develop cyanosis during the first year of life. Some patients with mild or no RVOT obstruction are not cyanotic at birth ("pink TOF") and may exhibit signs and symptoms of pulmonary overcirculation similar to patients with a large VSD. As these patients grow, the subpulmonary infundibulum becomes progressively obstructive and cyanosis ensues (16).

Surgical repair of TOF is usually performed during the first year of life, often during the first six months (17). A typical repair includes patch closure of the VSD and relief of the RVOT obstruction using a combination of resection of obstructive muscle bundles and an overlay patch. When the pulmonary valve annulus is moderately or severely hypoplastic, the RVOT patch extends across the pulmonary valve into the main pulmonary artery, resulting in pulmonary regurgitation. In patients with TOF and pulmonary atresia, or when a major coronary artery crosses the RVOT, a conduit — either a homograft or a prosthetic tube — is placed between the RVOT and the pulmonary arteries. The results of surgical repair of TOF have improved dramatically since the introduction of open-heart surgery. Early mortality is currently less than 2%, and the 20-year survival nears 90% (18–20). The majority of these patients, however, have residual hemodynamic abnormalities, primarily due to RV volume load from chronic pulmonary regurgitation. Other sequelae include RV hypertension from RVOT or pulmonary arterial obstruction(s), RV dysfunction, tricuspid regurgitation, LV volume load from a residual shunt such as a patch margin VSD, and aortic dilatation. Conduction and rhythm abnormalities are another major source of late morbidity and mortality in this growing patient population (21–27).

## MRI evaluations

TOF is the most frequent diagnosis among patients referred for CMR evaluation at Children's Hospital Boston. Unlike infants in whom echocardiography generally provides all the necessary diagnostic information for surgical repair (6, 28), MRI assumes an increasing role in adolescents and adults with TOF in whom the acoustic windows are frequently limited (29). CMR is useful in both pre- and post-operative assessment of TOF but the focus of the examination is different.

### Pre-operative MRI

In most patients with unrepaired TOF, the central question for the CMR examination is to delineate all sources of pulmonary blood flow—pulmonary arteries, aorto-pulmonary collaterals, and the ductus arteriosus. Several studies have shown that spin echo and 2D gradient echo cine MRI techniques provide excellent imaging of the central pulmonary arteries and major aorto-pulmonary collaterals (30–33). However, these MRI techniques require relatively long scan times for complete anatomical coverage, and small vessels (<2 mm) may not be detected. Furthermore, these 2-dimensional techniques are not optimal for imaging long and tortuous blood vessels, some of which arise from the brachiocephalic arteries or from the abdominal aorta. Gd-enhanced 3D MRA is ideally suited to image these vessels (Figs. 1 and 2). Compared with conventional X-ray angiography, MRA has been shown to be highly accurate in depicting all sources of pulmonary blood supply in patients with complex pulmonary stenosis or atresia, including infants with multiple small aorto-pulmonary collaterals (34).

An ECG-triggered gradient echo cine MRI, preferably steady-state free precession (SSFP), is used to assess ventricular dimensions and function, the right ventricular outflow tract valve function. When the origins and proximal course of the left and right coronary arteries are not known from other imaging studies, they should be imaged either by a gradient echo sequence designed for coronary imaging or by a fast spin echo sequence. Particular attention is paid to the exclusion of a major coronary artery crossing the right ventricular outflow tract.

### Post-operative MRI

CMR has been used extensively for assessment of post-operative TOF patients of all ages, but its greatest clinical utility is in adolescents and adults (29, 35). Quantitative assessment of RV and LV dimensions and function is a key element of CMR evaluation in patients with repaired TOF. The degree of RV dysfunction is an important determinant of clinical status late after TOF and is also closely associated with LV dysfunction, likely through ventricular-ventricular interaction (Fig. 3) (36). Many studies have shown that the degree of pulmonary regurgitation measured by velocity-encoded cine (VEC) MRI is closely associated with the degree of RV dilation (37–40). Another factor that
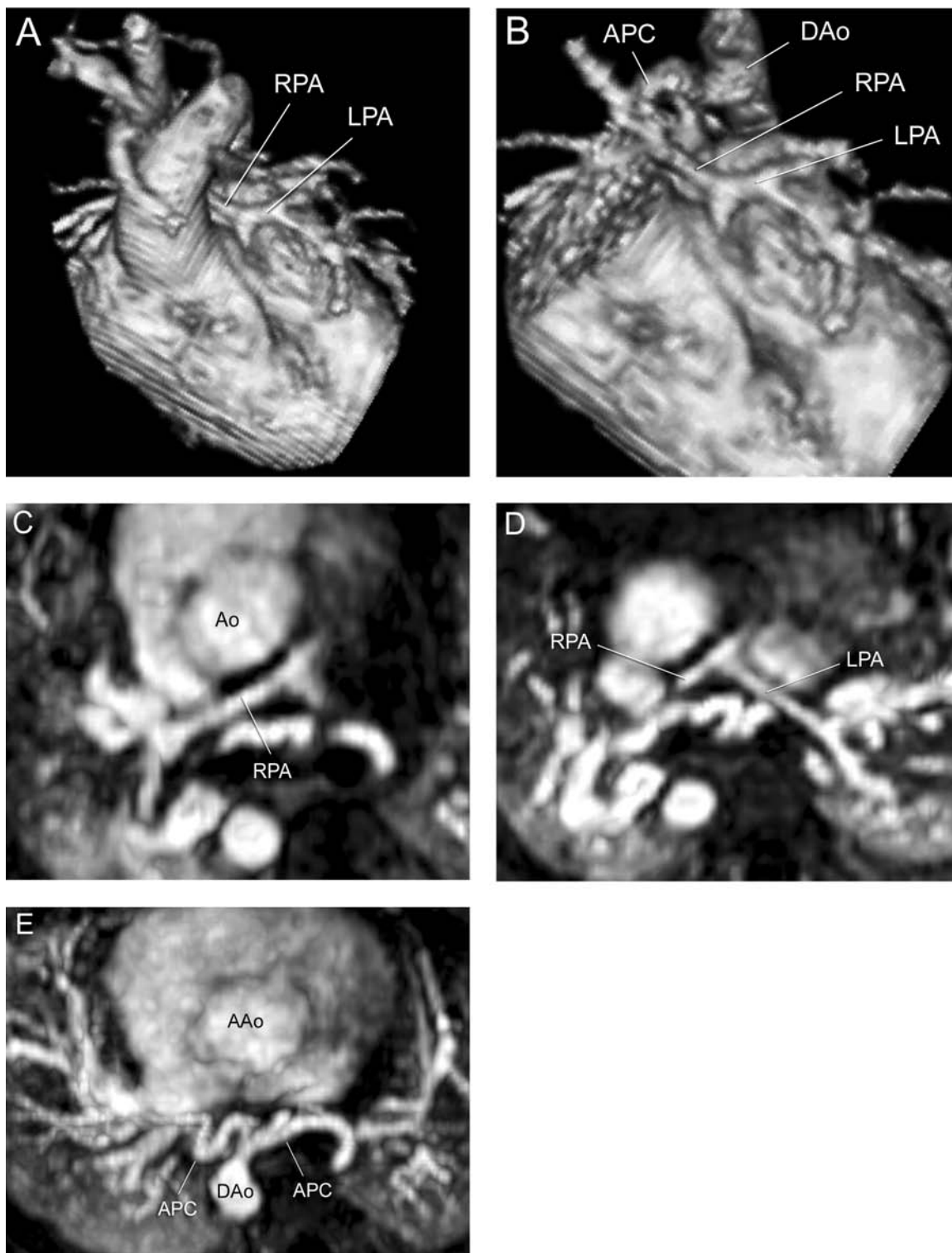
**Figure 1.** Sources of pulmonary blood supply in a newborn with TOF and pulmonary atresia evaluated by Gd-enhanced 3D magnetic resonance angiography (MRA). **A.** 3D reconstruction showing hypoplastic central pulmonary arteries (LPA = left pulmonary artery, RPA = right pulmonary artery); **B.** The aorta was removed to expose the distal right pulmonary artery (RPA). Note an aorto-pulmonary collateral (APC) vessel from the descending aorta (DAo) connecting to the distal RPA; **C.** Subvolume maximum intensity projection (MIP) image in the axial plane showing hypoplastic RPA; **D**. Subvolume maximum intensity projection (MIP) image in the axial plane showing hypoplastic LPA; **E**. Subvolume maximum intensity projection (MIP) image in the axial plane showing a large aorto-pulmonary collateral vessel (APC) arising from the descending aorta (DAo) and splitting into two large branches, one to the left lung and one to the right lung.
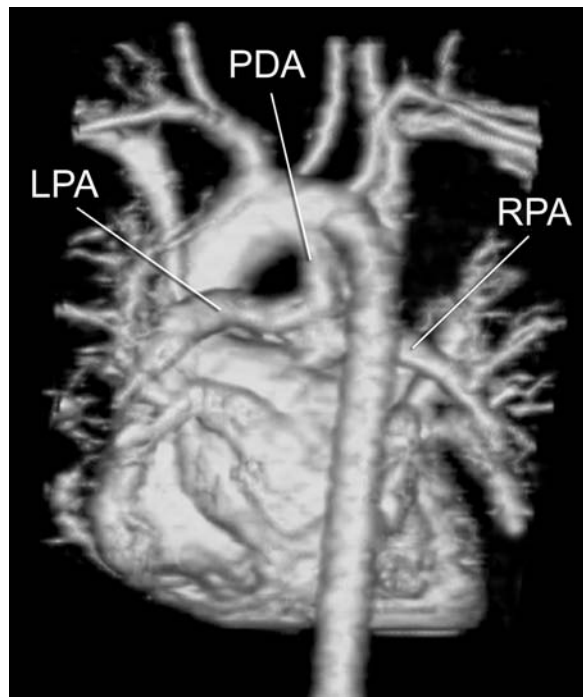
**Figure 2.** 3D reconstruction of Gd-enhanced MRA in a 1.3 kg new-born with heterotaxy syndrome, dextrocardia, TOF and pulmonary atresia. Pulmonary blood supply is exclusively through a patent ductus arteriosus (PDA), which supplies good-sized confluent left pulmonary artery (LPA) and right pulmonary artery (RPA).
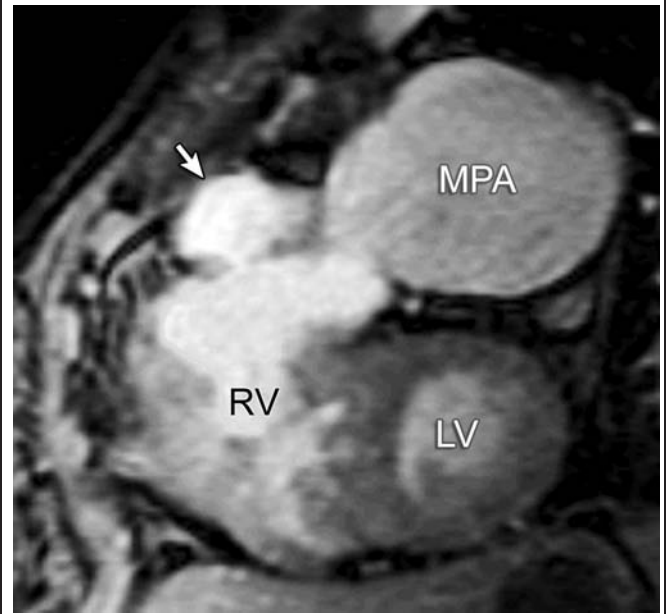


**Figure 4.** ECG-gated gradient echo cine MR showing an aneurysm of the right ventricular outflow tract (arrow) after TOF repair. LV = left ventricle; MPA = main pulmonary artery; RV = right ventricle.

affects RV function is the presence and extent of an aneurysm in the RVOT (Fig. 4) (41). Taken together with clinical assessment and electrophysiological data, information derived from CMR on pulmonary regurgitation fraction, RV and LV dimensions and function, presence and extent of a RVOT aneurysm, and presence of branch pulmonary artery stenosis is used to direct clinical care in patients with repaired TOF. Another technique that is increasingly being used in patients with repaired CHD is

post-gadolinium myocardial delayed enhancement (MDE) for assessment of myocardial fibrosis (Fig. 5) (42). The clinical significance of positive MDE in patients with repaired TOF awaits further study.
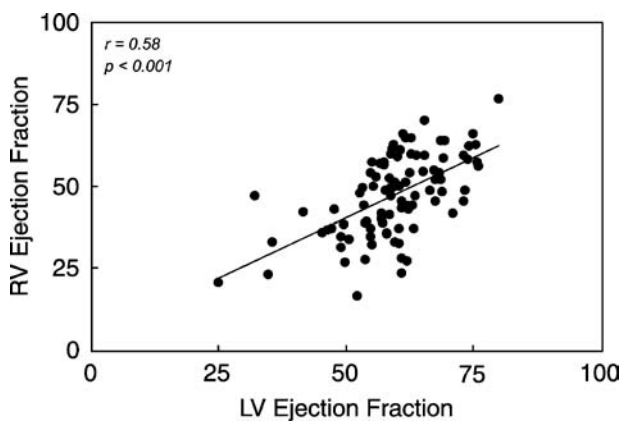


**Figure 3.** Correlation between RV and LV ejection fractions in 100 patients evaluated by CMR at a median of 21 years after TOF repair (36).



**Figure 5.** Myocardial delayed enhancement imaging in post-operative TOF. Images were acquired in the short-axis plane approximately 12 minutes after intravenous administration of gadopentetate dimeglumine (0.2 mmol/kg). Note the enhanced signal in the area of the right ventricular outflow tract patch (arrows).

The goals of the CMR examination, therefore, include quantitative assessment of left and right ventricular volumes, mass, stroke volumes, and ejection fraction, imaging the anatomy of the right ventricular outflow tract, pulmonary arteries, aorta, and aorto-pulmonary collaterals, and quantification of pulmonary regurgitation, tricuspid regurgitation, cardiac output, and pulmonary-to-systemic flow ratio. These objectives can be achieved by the following protocol:

- 3-plane localizing images;
- ECG-gated cine SSFP sequences in the 2-chamber and 4-chamber planes;
- ECG-gated cine SSFP sequence in the short-axis plane across the ventricles from base-to-apex (12 slabs with adjustment of the slice thickness and the inter-slice space to completely cover both ventricles) for quantitative assessment of ventricular dimensions and function;
- ECG-gated cine SSFP sequence parallel to the right ventricular outflow tract and pulmonary arteries;
- Gadolinium-enhanced 3-dimensional MRA
- ECG-gated velocity-encoded cine (VEC) MRI sequences perpendicular to the main pulmonary artery (± branch pulmonary arteries), ascending aorta, and AV valves;
- Post-gadolinium delayed myocardial enhancement may be used to evaluate the presence of scar tissue.

SSFP cine sequences are acquired with breath-holding whenever possible. Fast (turbo) spin echo with double inversion recovery sequence may be used to minimize artifacts from metallic implants, when present. Under optimal conditions, the above study protocol requires 60 minutes to complete. The use of sensitivity encoding or other parallel processing imaging techniques can further shorten the examination time.

# TRANSPOSITION OF THE GREAT ARTERIES

Transposition of the great arteries (TGA) is defined as discordant connections between the ventricles and the great arteries; the aorta arises from the RV, and the pulmonary artery arises from the LV. There are several anatomical types of TGA, depending on the viscero-atrial situs (solitus or inversus) and the type of ventricular loop (D or L) (43). The most common type of TGA is in viscero-atrial situs solitus (S), ventricular D-loop (D), and dextro malposition of the aortic valve relative to the pulmonary valve (D). This anatomical arrangement can be summarized as {S,D,D} TGA. Note that the term "D-TGA" is non-specific as the "D" might relate to the ventricular loop or to the spatial position of the aortic and pulmonary valves. This ambiguity can be avoided by using the term *D-loop TGA*. The incidence of D-loop TGA is estimated at 303 per million live births (1). The principal physiological abnormality in D-loop TGA is that systemic venous blood returns to the aorta and oxygenated pulmonary venous blood returns to the lungs, resulting in profound hypoxemia. Consequently, survival is dependent on communication(s) that allow mixing of blood between the systemic and pulmonary circulations. The most common sites of shunting are through the

ductus arteriosus, ASD, and/or VSD. Associated anomalies include VSD in ~45% of patients, coarctation or interrupted aortic arch in ~12%, pulmonary stenosis in ~5%, RV hypoplasia in ~4%, juxtaposition of the atrial appendages in ~2%, and other anomalies in 1% of patients or less, each (44).

Surgical management of D-loop TGA in the 1960s and 1970s consisted mostly of an atrial switch procedure—the Senning or Mustard operations. In both procedures, the systemic and pulmonary venous blood returns are redirected within the atria so that the pulmonary venous blood reaches the tricuspid valve, RV, and aorta, whereas the systemic venous blood reaches the mitral valve, LV, and pulmonary arteries. The main technical difference between these procedures is that in the Mustard operation the surgeon uses pericardium to redirect the blood flow, and in the Senning operation the surgeon uses native atrial tissue (45). The main drawbacks of the atrial switch operations include RV (systemic ventricle) dysfunction, sinus node dysfunction, atrial arrhythmias, obstruction of the systemic and/or pulmonary venous pathways, and baffle leaks (46–48). Beginning in the late 1970s and rapidly gaining popularity in the 1980s, the arterial switch operation (ASO) largely replaced the atrial switch procedures (49, 50). The advantages of the ASO over the atrial switch procedures include reestablishment of the LV as the systemic ventricle and avoidance of extensive suture lines in the atria. Recent data on late outcome of the ASO continues to show excellent overall survival with low morbidity (51–56). The Rastelli operation is another surgical option for patients with an associated subvalvar and valvar pulmonary stenosis and a VSD. It consists of patch closure of the VSD to the aortic valve and placement of a conduit between the RV and the pulmonary arteries.

The second most common type of TGA is in viscero-atrial situs solitus (S), L-ventricular loop (L), and levo-malposition of the aortic valve relative to the pulmonary valve (L). This anatomical arrangement can be summarized as {S,L,L} TGA or L-loop TGA (57–60). It is also known as "physiologically corrected" TGA because the systemic venous return reaches the pulmonary circulation through the right-sided LV and the pulmonary venous return reaches the aorta through the left-sided RV. Associated anomalies include tricuspid valve abnormalities (e.g., Ebstein anomaly), RV hypoplasia, VSD, subvalvar and valvar pulmonary stenosis, as well as conduction abnormalities, including complete heart block. Outcome is determined primarily by the associated lesions and RV (the systemic ventricle) function (57–60).

## *MRI evaluations*

CMR is seldom requested for pre-operative assessment of infants with D-loop TGA because echocardiography usually provides all necessary diagnostic information (44). In postoperative TGA, CMR assumes an increasing role due to its ability to non-invasively evaluate most clinically relevant issues (61–69).

### Post-operative atrial switch

The goals of CMR evaluation of postoperative atrial switch include: (1) quantitative evaluation of the size and function of the

systemic RV (62); (2) imaging of the systemic and pulmonary venous pathways for obstruction and/or baffle leak(s); (3) assessment of tricuspid valve regurgitation; (4) evaluation of the left and right ventricular outflow tracts for obstruction; and (5) detection of aorto-pulmonary collateral vessels and other associated anomalies. In patients with RV dysfunction, post-gadolinium delayed myocardial enhancement can be used to detect myocardial fibrosis. The response of the systemic RV to pharmacological stress (dobutamine) or to exercise can be tested by CMR, but the clinical utility of this information awaits further study (67, 69). These objectives can be achieved by the following protocol:
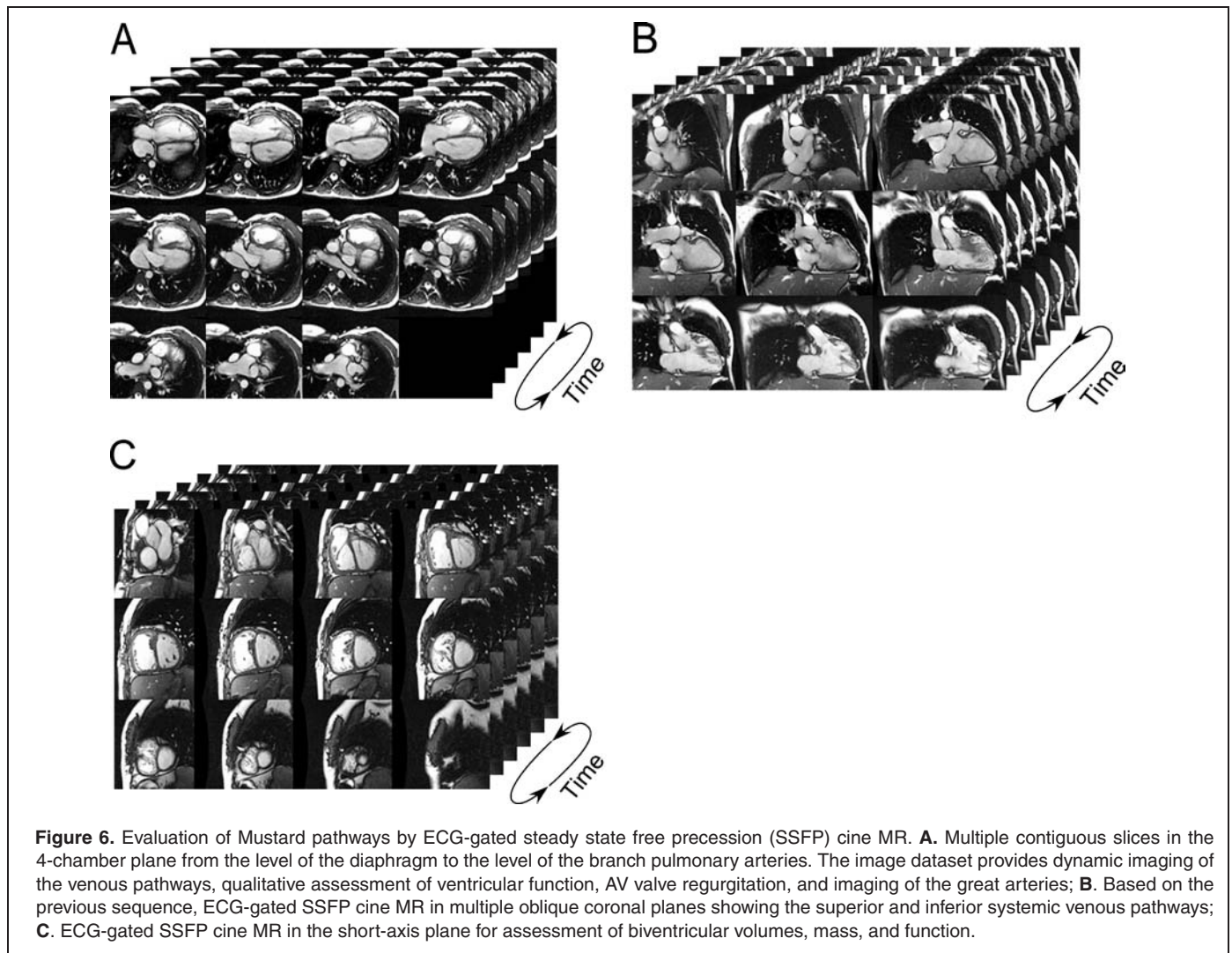
- 3-plane localizing images;
- ECG-gated cine SSFP sequence in the 4-chamber or axial planes with multiple contiguous slices from the level of the diaphragm to the level of the transverse arch (provides dynamic imaging of the venous pathways, qualitative assessment of ventricular function, AV valve regurgitation, and imaging of the great arteries) (Fig. 6A);
- Based on the previous sequence, ECG-gated cine SSFP sequence in multiple oblique coronal planes parallel to the SVC and IVC pathways to image them in their long-axis (Fig. 6B);
- ECG-gated cine SSFP sequence in the short-axis plane across the ventricles from base-to-apex (12 slabs) for quantitative assessment of ventricular dimensions and function (Fig. 6C);
- ECG-gated VEC MRI sequences perpendicular to the AV valves, main pulmonary artery, and the ascending aorta. Additional VEC MRI sequences may be obtained to evaluate specific areas suspected for obstruction (70);
- Gd-enhanced 3-dimensional MRA.

SSFP cine sequences are acquired with breath-holding whenever possible. Fast (turbo) spin echo with double inversion recovery sequence may be used to minimize artifacts from metallic implants and post-gadolinium delayed myocardial enhancement may be used to evaluate the presence of scar tissue (42).

### Postoperative arterial switch

The long-term concerns in patients after the ASO relate primarily to the technical challenges of the operation—transfer



**Figure 6.** Evaluation of Mustard pathways by ECG-gated steady state free precession (SSFP) cine MR. **A.** Multiple contiguous slices in the 4-chamber plane from the level of the diaphragm to the level of the branch pulmonary arteries. The image dataset provides dynamic imaging of the venous pathways, qualitative assessment of ventricular function, AV valve regurgitation, and imaging of the great arteries; **B**. Based on the previous sequence, ECG-gated SSFP cine MR in multiple oblique coronal planes showing the superior and inferior systemic venous pathways; **C**. ECG-gated SSFP cine MR in the short-axis plane for assessment of biventricular volumes, mass, and function.

**A. L. Dorfman and T. Geva**

**Figure 7.** 3D reconstruction of Gd-enhanced MRA in post-operative arterial switch operation.

from base-to-apex for quantitative assessment of ventricular dimensions and function;

- ECG-gated VEC MRI sequences perpendicular to the main and branch pulmonary arteries and the ascending aorta. Additional VEC MRI sequences may be obtained to evaluate specific areas suspected for obstruction (70); and
- Gd-enhanced 3-dimensional MRA.

SSFP cine sequences are acquired with breath-holding whenever possible. Fast (turbo) spin echo with double inversion recovery sequence may be used to minimize artifacts from metallic implants. Imaging of the coronary arteries is increasingly being incorporated into the study protocol to evaluate for stenosis. Pharmacological stress testing—either adenosine or dobutamine—for evaluation of myocardial ischemia and MDE for detection of myocardial fibrosis is increasingly being incorporated into the clinical imaging protocol in patients with repaired TGA.

## DOUBLE-OUTLET RIGHT VENTRICLE

Double-outlet right ventricle (DORV) is defined as a specific type of ventriculo-arterial alignment in which both great vessels arise from the RV or from the infundibulum. The incidence of DORV is estimated at 127 per million live births (1). It is important to recognize the wide spectrum of anatomic and physiologic variations that share this type of ventriculo-arterial alignment. In fact, the clinical course and management of patients with DORV are dictated in large part by the size and location of the ventricular septal defect in relation to the semilunar valves, the anatomy of the infundibulum and the semilunar valves, the position of the infundibular septum, the size of the LV and RV sinuses, and the anatomy of the AV valves. The LV can be normal sized, hypoplastic, or absent. The RV is usually good sized but in rare circumstances it can be hypoplastic or even absent (double-outlet infundibulum). Both semilunar valves can be patent but stenosis or atresia is relatively common. The presence of a straddling mitral or tricuspid valve is particularly important with regard to surgical planning. Examples of some of the common anatomic-physiologic variations encountered in patients with DORV include:

- VSD physiology: DORV with subaortic VSD and no pulmonary stenosis,
- Tetralogy of Fallot physiology: DORV with sub-aortic VSD and pulmonary stenosis,
- Transposition of the great arteries physiology: DORV with subpulmonary VSD, with or without systemic (aortic) outflow obstruction (Taussig-Bing type DORV),
- Single-ventricle physiology: DORV with mitral atresia, unbalanced AV canal, or severe hypoplasia of one of the ventricular sinuses (often in association with heterotaxy syndrome).

The ultimate goal of surgical management of DORV is to align the LV with the systemic outflow and the RV with the pulmonary outflow. In DORV with a subaortic VSD, the LV can be aligned with the aorta by placing a patch on the right ventricular

of the coronary arteries from the native aortic root to the neo-aortic root (native pulmonary root) and the transfer of the pulmonary arteries anterior to the neo-ascending aorta (Fig. 7). Consequently, the goals of CMR evaluation of postoperative arterial switch include: (1) evaluation of global and regional LV and RV size and function; (2) evaluation of the left and right ventricular outflow tracts for obstruction; (3) qualitative estimation of RV systolic pressure based on the configuration of the interventricular septum; (4) imaging of the great vessels with emphasis on evaluation of the pulmonary arteries for stenosis and the aortic root for dilatation; and (5) detection of aorto-pulmonary collaterals and other associated anomalies. The role of myocardial perfusion and viability imaging in this population deserves further study. The above objectives can be achieved by the following protocol:

- 3-plane localizing images;
- ECG-gated cine SSFP sequence in the axial plane with multiple contiguous slices from the mid-ventricular level to the level of the transverse arch (provides axial dynamic imaging of the outflow tracts and the great arteries, qualitative assessment of ventricular function, and AV valve regurgitation);
- ECG-gated cine SSFP sequence in the coronal and/or oblique sagittal planes parallel to the left and right ventricular outflow tracts;
- ECG-gated cine SSFP sequences in the 2- and 4-chamber planes followed by a short-axis stack across the ventricles

aspect of the defect, leaving the aortic valve on the left ventricular side. Resection of RVOT obstruction, with or without an outflow patch, may be necessary in patients with subvalvar or valvar pulmonary stenosis, analogous to TOF repair. In DORV with a subpulmonary VSD (Taussig-Bing variety), the VSD is closed with a patch that directs the blood from the LV to the pulmonary valve accompanied by an arterial switch procedure. More complex forms of DORV with heterotaxy syndrome, se-

vere hypoplasia or absence of one of the ventricular sinuses, major straddling of an AV valve, or mitral atresia are palliated as a single ventricle with an eventual Fontan procedure.

Late complications in patients with repaired DORV are relatively common and vary with their underlying anatomy, physiology, and surgical repair. Subaortic stenosis can develop after the LV is baffled to the aorta (71). The complications after repair of DORV with pulmonary outflow tract obstruction are
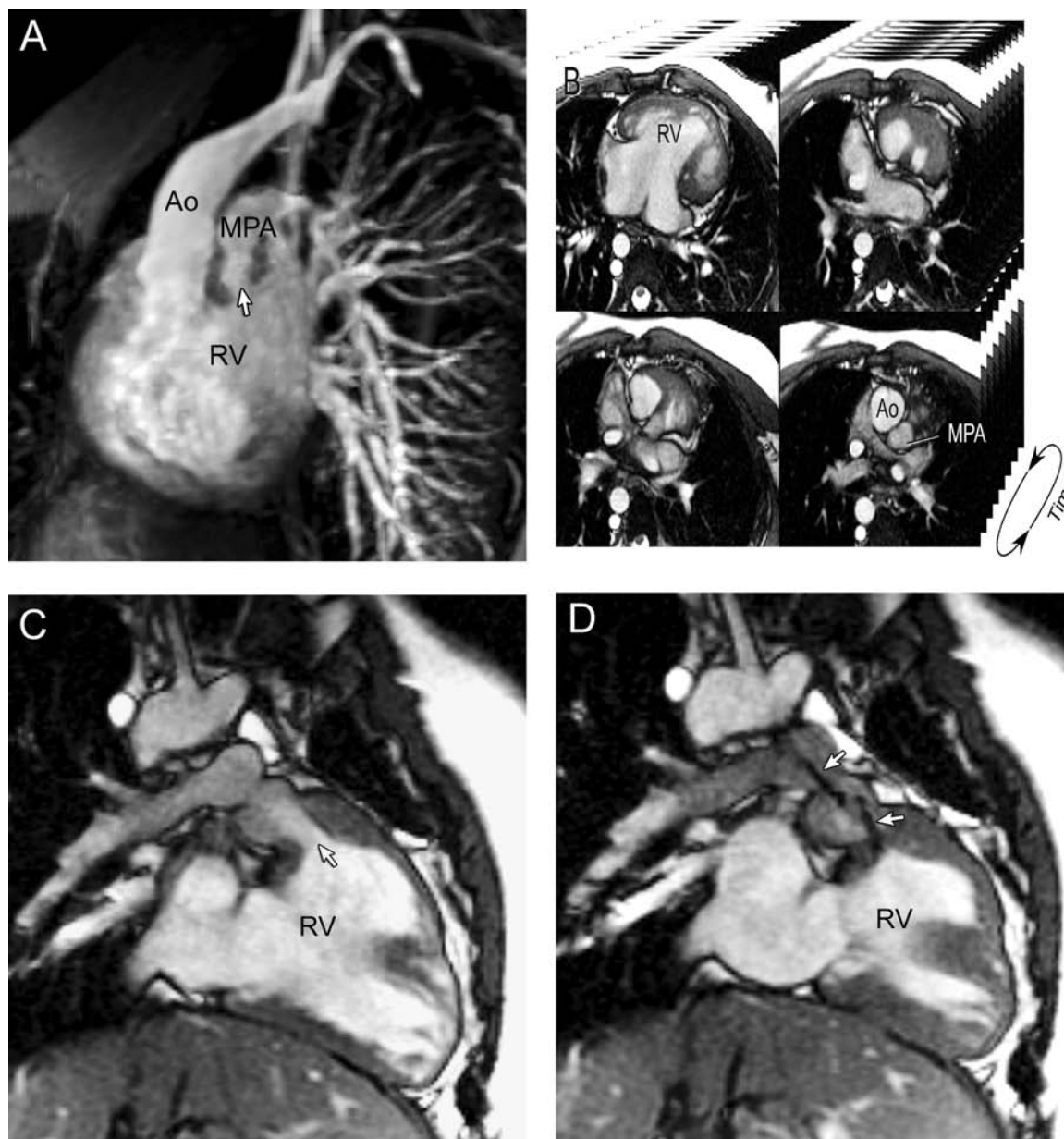


**Figure 8.** MRI evaluation of heterotaxy syndrome, common AV canal, and double-outlet right ventricle with pulmonary stenosis. **A**. Subvolume MIP image of Gd-enhanced 3D MRA showing origin of the aorta (Ao) and main pulmonary artery (MPA) from the right ventricle (RV). Note the subvalvar pulmonary stenosis (arrow); **B**. Multislice ECG-gated SSFP cine MR in the axial plane. The left upper slice shows the RV-dominant common AV canal. The right upper slice shows the subaortic and subpulmonary conus. The right lower slice shows the great arteries with the larger aorta (Ao) to the right and anterior relative to the smaller main pulmonary artery (MPA); **C**. Diastolic frame of an ECG-gated SSFP cine MR in an oblique coronal plane showing the narrowed subpulmonary conus (arrow); **D**. Systolic frame in the same location as C showing two jets (arrows)—the inferior jet is due to subvalvar stenosis and the superior jet due to pulmonary valve stenosis.
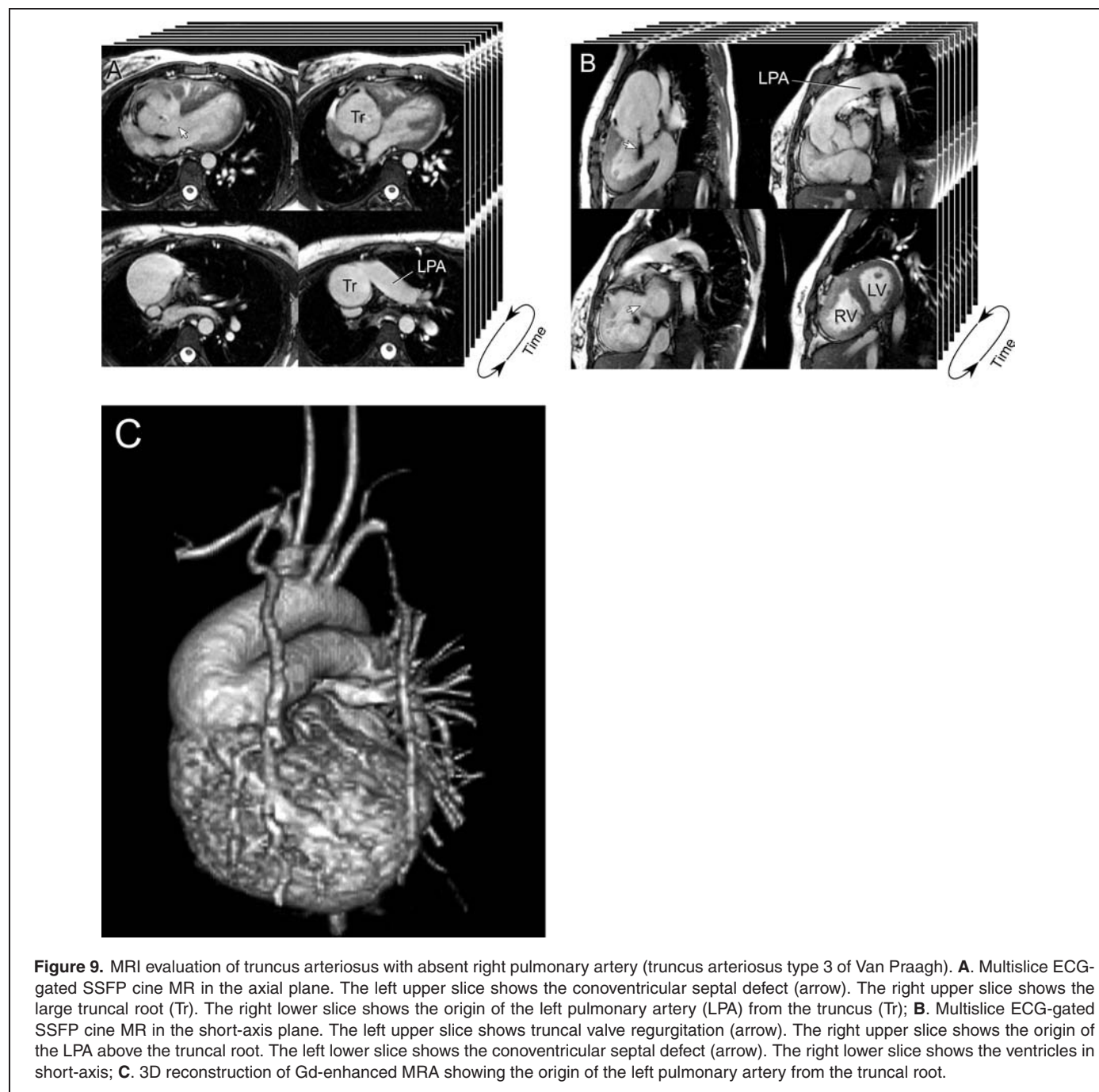
**A. L. Dorfman and T. Geva**

similar to those seen after TOF repair, including chronic pulmonary regurgitation, dilation and dysfunction of the RV, and arrhythmia. Aortic arch obstruction can be found in patients after coarctation or interrupted aortic arch repair. Those who undergo an arterial switch operation may have the same problems described above for this procedure.

## Pre-operative MRI

Because echocardiography is usually sufficient for diagnosis and surgical planning in most newborns or infants with DORV,

CMR is seldom requested for preoperative evaluation in this age group. Exceptions include patients with complex anomalies of the aortic arch, pulmonary arteries, aorto-pulmonary collaterals, and systemic or pulmonary venous anomalies that are not completely delineated by echocardiography. Several investigators demonstrated the use of CMR for the assessment of the relationship between the great vessels and the VSD as well as the position of the great vessels in relation to the conal septum (72–76).

The imaging strategy is tailored to address the specific clinical question(s). In general, gadolinium-enhanced 3D MRA is particularly helpful for evaluation of great vessel anatomy (Fig. 8).



**Figure 9.** MRI evaluation of truncus arteriosus with absent right pulmonary artery (truncus arteriosus type 3 of Van Praagh). **A**. Multislice ECG-gated SSFP cine MR in the axial plane. The left upper slice shows the conoventricular septal defect (arrow). The right upper slice shows the large truncal root (Tr). The right lower slice shows the origin of the left pulmonary artery (LPA) from the truncus (Tr); **B**. Multislice ECG-gated SSFP cine MR in the short-axis plane. The left upper slice shows truncal valve regurgitation (arrow). The right upper slice shows the origin of the LPA above the truncal root. The left lower slice shows the conoventricular septal defect (arrow). The right lower slice shows the ventricles in short-axis; **C**. 3D reconstruction of Gd-enhanced MRA showing the origin of the left pulmonary artery from the truncal root.

Intracardiac anatomy is assessed by SSFP cine MRI and by fast (turbo) spin echo with double inversion recovery. More recently, Sorensen et al. described the use of free breathing ECG triggered, navigator-gated, isotropic 3D SSFP sequence that holds promise for assessment of both intra- and extra-cardiac anatomy (77). Although the quality of the images obtained in children under 7 years was inferior to those in older patients, further refinements may prove this technique helpful for assessment of complex intracardiac anatomy (77).

### Post-operative MRI

The role of CMR after DORV repair increases as patients grow and their acoustic windows become progressively more limited. The examination strategy is tailored based on the underlying anatomy, the operation(s) performed and the specific clinical and other diagnostic findings. Although no single generic imaging protocol covers all possible scenarios after DORV repair, certain patterns are recognized. Patients with a "TOF-like" DORV repair have similar long-term sequelae as those after TOF repair, and the CMR examination protocol is comparable (see previous section). Similarly, in those with Taussig-Bing type DORV, the postoperative issues are similar to those encountered after the arterial switch operation for TGA (see previous section). The importance of modifying the examination protocol to address anatomic and functional abnormalities specific to the individual patient cannot be overstated. This requires on-line evaluation of the imaging data since previously unsuspected abnormalities may only be detected during the scan.

## TRUNCUS ARTERIOSUS

Truncus arteriosus is an uncommon conotruncal anomaly with a reported incidence of 94 per million live births (1). It is defined by the presence of a single artery arising from the heart with a single semilunar valve, giving rise to the coronary arteries, aorta, and at least one branch pulmonary artery. Van Praagh and Van Praagh (78) modified the original classification of Collett and Edwards (79):

- Type I: The branch pulmonary arteries arise from a short main pulmonary artery;
- Type II: The branch pulmonary arteries arise directly from the arterial trunk through separate orifices;
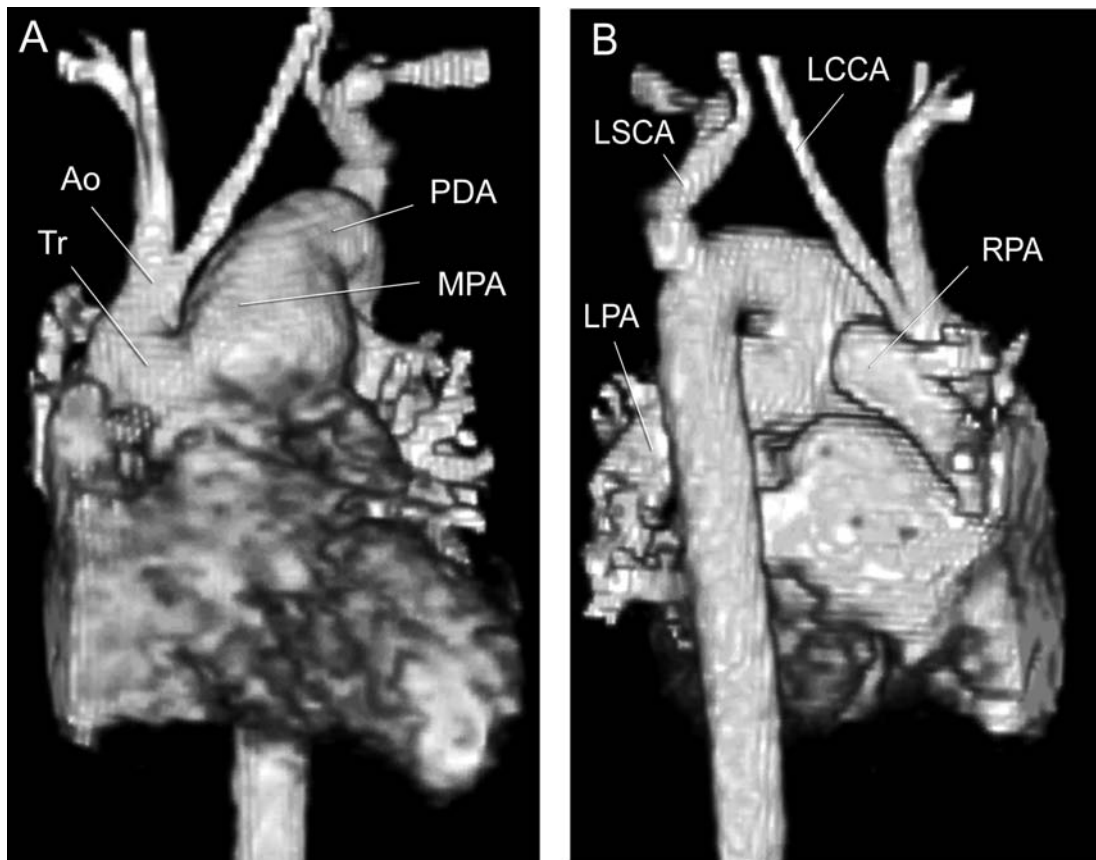


**Figure 10.** 3D reconstruction of Gd-enhanced MRA in a newborn with truncus arteriosus and type B interrupted aortic arch (truncus type 4 of Van Praagh). **A**. Anterior view showing the ascending aorta (Ao), which gives rise to the right innominate and to the left common carotid arteries. The main pulmonary artery (MPA) continues as a large patent ductus arteriosus (PDA); **B**. Posterior view showing the interruption between the left common carotid artery (LCCA) and the left subclavian artery (LSCA), which arises from the proximal descending aorta.

- Type III: Only one branch pulmonary artery arises from the ascending segment of the trunc. Collateral vessels usually supply the contralateral lung;
- Type IV: Truncus arteriosus with aortic arch hypoplasia, coarctation, or interruption (usually type B distal to the left common carotid artery). In this anatomic variation there is usually a well-formed main pulmonary artery and a small ascending aorta.

In the majority of cases there is a subtruncal VSD over which the truncal valve sits, similar to TOF. Rarely, the ventricular septum is intact. The conal septum is usually absent and the truncal valve is in direct fibrous continuity with the mitral valve. In rare circumstances, the truncal valve may be supported by a complete infundibulum and relate exclusively to the RV. The truncal valve is most commonly tricommissural, followed by bicommissural morphology, and least common is a quadricommissural valve. The valve can be thickened and redundant with stenosis, regurgitation, or both. Associated cardiovascular and non-cardiac anomalies are frequent. Examples of associated cardiovascular anomalies include multiple VSDs, partial and complete atrioventricular canal defects, mitral atresia, mitral stenosis, aortic atresia, hypoplastic left ventricle, double-inlet left ventricle, tricuspid atresia, straddling tricuspid valve, Ebstein malformation, heterotaxy syndrome, aberrant origin of the right or left subclavian artery, coarctation of the aorta, secundum atrial septal defect, partially and totally anomalous pulmonary venous connections, left superior vena cava to coronary sinus, retroaortic innominate vein, and left pulmonary artery sling (80). Various non-cardiac anomalies have been described with truncus arteriosus. DiGeorge syndrome, velocardiofacial syndrome, and chromosome 22q11 deletion are frequently associated. A large series found the 22q11 deletion in 34.5% of patients with truncus arteriosus (81).

Most patients with truncus arteriosus are diagnosed early in life and echocardiography is sufficient for diagnosis and surgical planning in almost all. Surgical repair usually follows the diagnosis. Typically, the VSD is closed with a patch so that the truncal valve is aligned with the LV (becoming the neo-aortic valve), and the pulmonary arteries are detached from the arterial trunk and connected to the RV with a valved homograft. Surgical repair of the truncal valve for stenosis or regurgitation is uncommon during the initial repair. Surgical mortality is low and has improved with the overall advances in surgical management of infants. The use of a non-growing homograft in infancy makes additional operations inevitable as patients grow. Important residual lesions after truncus arteriosus repair include progressive stenosis and regurgitation of the RV-to-pulmonary artery homograft, branch pulmonary artery stenosis, and regurgitation or stenosis of the neo-aortic (truncal) valve. Aortic arch obstruction can complicate the course of patients with coarctation or interrupted aortic arch repair.

## *Pre-operative MRI*

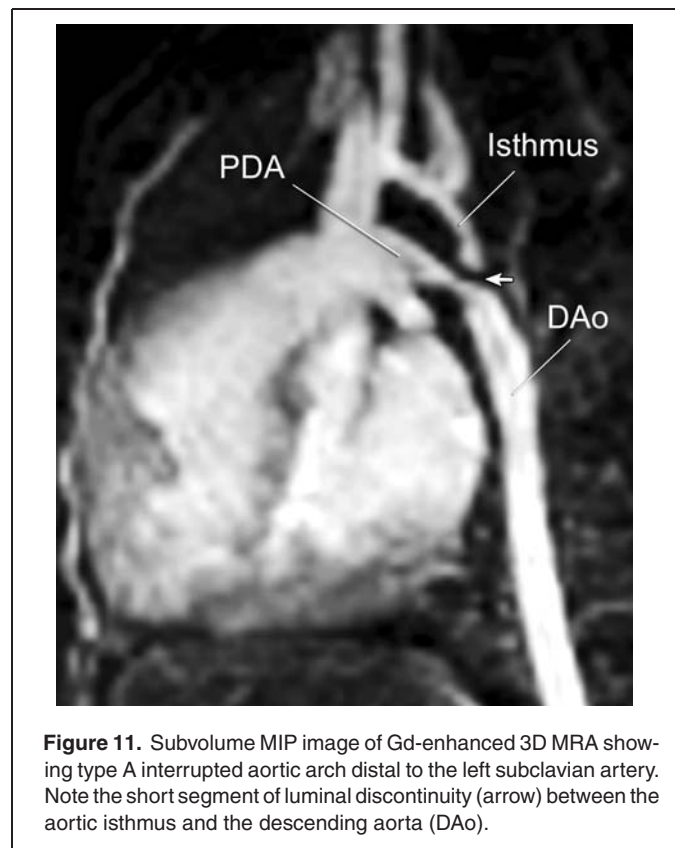CMR is rarely requested for pre-operative evaluation in an infant with truncus arteriosus because echocardiography is almost always adequate (82). Exceptions include complex aortic arch or pulmonary venous anomalies that require further delineation and the occasional older patient with an unrepaired truncus arteriosus (Fig. 9).

## *Post-operative MRI*

The role of CMR in patients with repaired truncus arteriosus increases with their age. The anatomic and functional issues in these patients are similar to those encountered in patients with repaired TOF, especially in those with TOF and pulmonary atresia. In addition, neo-aortic valve dysfunction and aortic arch obstruction are additional issues that may require investigation. Therefore, the goals of the CMR examination after truncus repair include: (1) quantitative assessment of left and right ventricular volumes, function, and mass; (2) measurements of pulmonary and neo-aortic valve regurgitation; (3) imaging of the right ventricular outflow tract, the homograft, and the branch pulmonary arteries; (4) assessment of residual shunts; and (5) imaging of the aortic arch and isthmus. These objectives can be achieved with modifications of the protocol described above for TOF and individualized for the patient's anatomic and hemodynamic issues.

## INTERRUPTED AORTIC ARCH

Interruption of the aortic arch (IAA) is an uncommon congenital cardiovascular malformation characterized by anatomic



**Figure 11.** Subvolume MIP image of Gd-enhanced 3D MRA showing type A interrupted aortic arch distal to the left subclavian artery. Note the short segment of luminal discontinuity (arrow) between the aortic isthmus and the descending aorta (DAo).
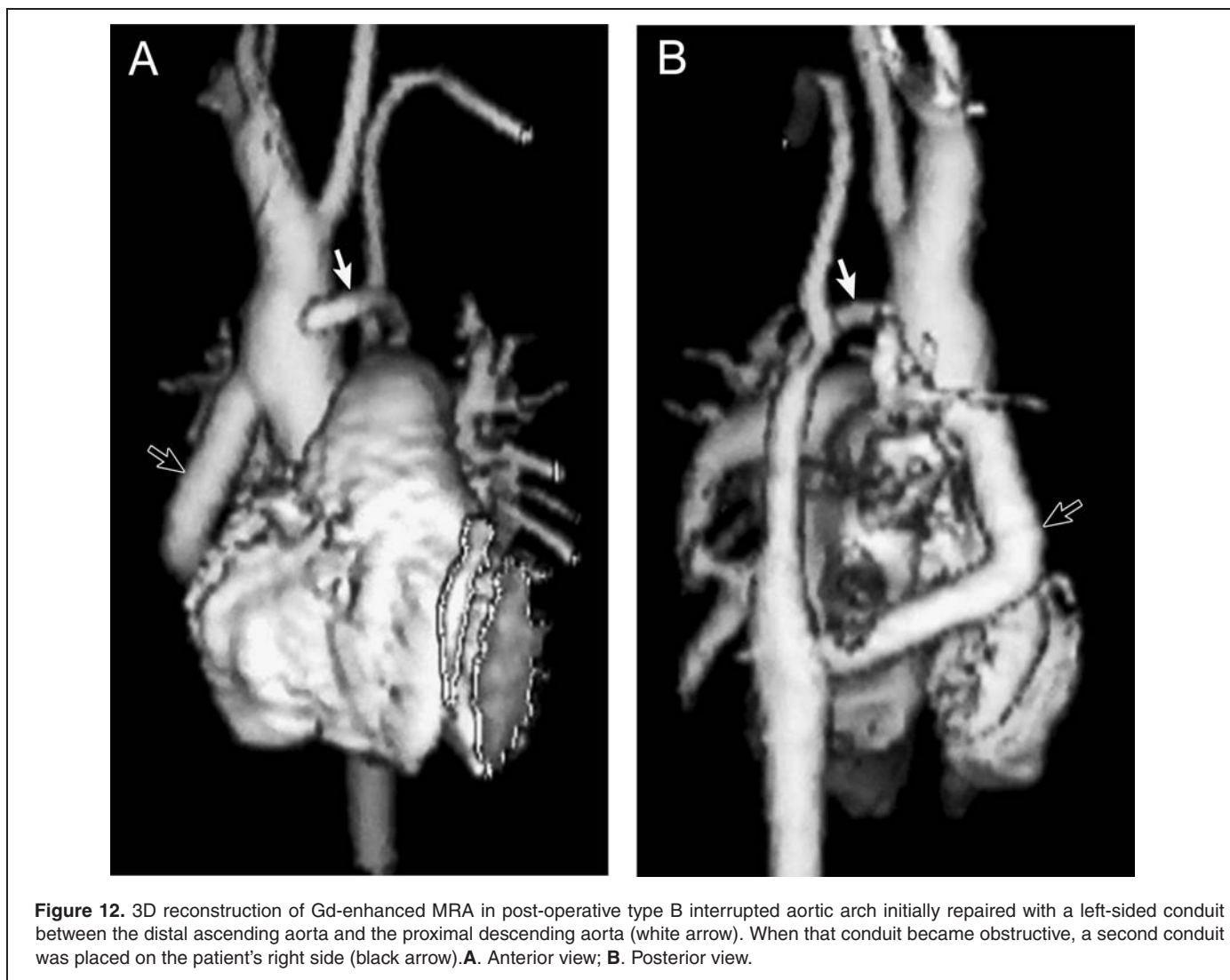
discontinuity between segments of the aortic arch. The prevalence of IAA is 19 per million live births, or 1.3% of infants with congenital heart disease in the New England Regional Infant Cardiac Program (83). This condition should be distinguished from aortic arch atresia where there is anatomic continuity between the arch segments through a fibrous strand, but the aortic lumen is completely obstructed. Because of their identical hemodynamic consequences, both conditions will be discussed together.

The classification proposed by Celoria and Patton in 1959 is widely used to date (84). Type A denotes interruption distal to the left subclavian artery; type B between the left common carotid and the left subclavian arteries; and type C between the common carotid arteries. Type B is the most common anatomic variation accounting for approximately 62% of IAA cases, type A for 37%, and type C for 1%. Other morphologic variations associated with IAA have been described. Aberrant origin of the right subclavian artery from the proximal descending aorta is found in roughly 50% of patients with type B IAA but only in a minority of those with type A interruption. Other rare variations include interruption of a right aortic arch (85) and interruption of a cervical arch (86).

Survival of patients with IAA depends on a patent ductus arteriosus. Intravenous administration of prostaglandin E begins immediately once the diagnosis is suspected and is followed by surgical repair. In most institutions, the preferred surgical approach is direct anastomosis of the interrupted (or atretic) aortic segments. When the distance between the interrupted aortic arch segments is large, homograft augmentation may be added to the arch reconstruction. The use of a tubular conduit to bridge between the arch segments is usually reserved for unusually long-segment interruptions or for re-operations. In patients with an associated VSD, the defect is closed at the time of the arch repair. In type B IAA with posterior malalignment of the conal septum and markedly hypoplastic left ventricular outflow tract, the VSD can be baffled to the pulmonary valve, the main pulmonary artery is transected and anastomosed to the ascending aorta, and a conduit (usually a valved homograft) is placed between the RV and the pulmonary arteries.



**Figure 12.** 3D reconstruction of Gd-enhanced MRA in post-operative type B interrupted aortic arch initially repaired with a left-sided conduit between the distal ascending aorta and the proximal descending aorta (white arrow). When that conduit became obstructive, a second conduit was placed on the patient's right side (black arrow).**A**. Anterior view; **B**. Posterior view.

**A. L. Dorfman and T. Geva**

## *MRI evaluation*

Echocardiography is usually adequate for pre-operative diagnosis of interrupted aortic arch and associated anomalies (87). CMR is used in selected patients in whom the anatomy is not clearly defined by echocardiography (88, 89). CMR assumes a larger role in patients with repaired IAA as they grow and their acoustic windows become restricted.

### Pre-operative MRI

The goal of the CMR examination is to delineate the anatomy of the aortic arch, and the branching pattern of the brachio-cephalic arteries (Fig. 10). It is important to fully evaluate the vascular anatomy to exclude any associated anomalies (e.g., systemic and pulmonary venous anomalies). Gadolinium-enhanced 3D MR angiography is the most robust and time-efficient technique to achieve these goals (Fig. 11) (89). The use of gradient echo cine and black blood imaging is tailored to the clinical and imaging issues of individual patients. Evaluation of intracardiac anatomy is usually not necessary since the information should be available from echocardiography.

### Post-operative MRI

The goal of the CMR examination after IAA surgery is to evaluate residual or recurrent anatomic and hemodynamic problems. Often, the focus is on imaging of the aortic arch and the repair site for evaluation of obstruction or aneurysm formation (Fig. 12). However, other abnormalities such as left ventricular outflow tract obstruction, aortic valve stenosis or regurgitation, residual VSD, left ventricular size and function, and other anomalies should be examined as well. The hemodynamic severity of residual or recurrent aortic arch obstruction can be assessed based on body surface area-adjusted smallest cross-sectional area of the aortic arch or isthmus (from Gd-enhanced 3D MRA) and the heart-rate-adjusted mean deceleration rate in the descending aorta (from PVC MRI) as described by Nielsen et al (90). These objectives can be achieved with the following protocol:

- 3-plane localizing images;
- ECG-gated cine SSFP sequences in the 2- and 4-chamber planes;
- ECG-gated cine SSFP sequence in the short-axis plane across the ventricles from base-to-apex (12 slabs with adjustment of the slice thickness and the inter-slice space to completely cover both ventricles) for quantitative assessment of ventricular dimensions and function;
- ECG-gated cine SSFP sequence parallel to the left ventricular outflow tract;
- ECG-gated cine SSFP sequence in the long axis of the aortic arch;
- Optional: ECG-gated fast (turbo) spin echo in the long axis of the aortic arch;
- Gadolinium-enhanced 3-dimensional MRA;
- ECG-gated VEC MRI sequences perpendicular to the ascending and descending aorta. Additional flow measurements are

obtained based on clinical relevance (e.g., assessment of aortic regurgitation).

## REFERENCES

1. Hoffman JI, Kaplan S. The incidence of congenital heart disease. J Am Coll Cardiol 2002;39:1890–1900.
2. Van Praagh R, Van Praagh S, Nebesar RA, Muster AJ, Sinha SN, Paul MH. Tetralogy of Fallot: underdevelopment of the pulmonary infundibulum and its sequelae. Am J Cardiol 1970;26:25–33.
3. Van Praagh R. Etienne-Louis Arthur Fallot and his tetralogy: a new translation of Fallot's summary and a modern reassessment of this anomaly. Eur J Cardiothorac Surg 1989;3:381–6.
4. Van Praagh R, Geva T, Kreutzer J. Ventricular septal defects: how shall we describe, name and classify them? J Am Coll Cardiol 1989;14:1298–9.
5. Flanagan MF, Foran RB, Van Praagh R, Jonas R, Sanders SP. Tetralogy of Fallot with obstruction of the ventricular septal defect: spectrum of echocardiographic findings. J Am Coll Cardiol 1988;11:386–95.
6. Need LR, Powell AJ, del Nido P, Geva T. Coronary echocardiography in tetralogy of fallot: diagnostic accuracy, resource utilization and surgical implications over 13 years. J Am Coll Cardiol 2000;36:1371–7.
7. Lu JH, Chung MY, Betau H, Chien HP, Lu JK. Molecular characterization of tetralogy of fallot within Digeorge critical region of the chromosome 22. Pediatr Cardiol 2001;22:279–84.
8. Marino B, Digilio MC, Toscano A, Anaclerio S, Giannotti A, Feltri C, de Ioris MA, Angioni A, Dallapiccola B. Anatomic patterns of conotruncal defects associated with deletion 22q11. Genet Med 2001;3:45–8.
9. Momma K, Takao A, Matsuoka R, Imai Y, Muto A, Osawa M, Takayama M. Tetralogy of Fallot associated with chromosome 22q11.2 deletion in adolescents and young adults. Genet Med 2001;3:56–60.
10. Boudjemline Y, Fermont L, Le Bidois J, Lyonnet S, Sidi D, Bonnet D. Prevalence of 22q11 deletion in fetuses with conotruncal cardiac defects: a 6-year prospective study. J Pediatr 2001;138:520–4.
11. Goldmuntz E, Geiger E, Benson DW. NKX2.5 mutations in patients with tetralogy of Fallot. Circulation 2001;104:2565–8.
12. Hokanson JS, Pierpont E, Hirsch B, Moller JH. 22q11.2 microdeletions in adults with familial tetralogy of Fallot. Genet Med 2001;3:61–4.
13. McElhinney DB, Krantz ID, Bason L, Piccoli DA, Emerick KM, Spinner NB, Goldmuntz E. Analysis of cardiovascular phenotype and genotype-phenotype correlation in individuals with a JAG1 mutation and/or Alagille syndrome. Circulation 2002;106:2567–74.
14. Masuda K, Nomura Y, Yoshinaga M, Nakamura M, Matsuda Y, Oku S, Miyata K. Inverted duplication/deletion of the short arm of chromosome 8 in two patients with tetralogy of Fallot. Pediatr Int 2002;44:534–6.
15. Marino B, Digilio MC, Grazioli S, Formigari R, Mingarelli R, Giannotti A, Dallapiccola B. Associated cardiac anomalies in isolated and syndromic patients with tetralogy of Fallot. Am J Cardiol 1996;77:505–8.
16. Geva T, Ayres NA, Pac FA, Pignatelli R. Quantitative morphometric analysis of progressive infundibular obstruction in tetralogy of Fallot. A prospective longitudinal echocardiographic study. Circulation 1995;92:886–92.
17. Kaulitz R, Jux C, Bertram H, Paul T, Ziemer G, Hausdorf G. Primary repair of tetralogy of fallot in infancy–the effect on growth of the pulmonary arteries and the risk for late reinterventions. Cardiol Young 2001;11:391–8.
18. Bacha EA, Scheule AM, Zurakowski D, Erickson LC, Hung J, Lang P, Mayer JE, Jr., del Nido PJ, Jonas RA. Long-term results after early primary repair of tetralogy of Fallot. J Thorac Cardiovasc Surg 2001;122:154–61.

19. Murphy JG, Gersh BJ, Mair DD, Fuster V, McGoon MD, Ilstrup DM, McGoon DC, Kirklin JW, Danielson GK. Long-term outcome in patients undergoing surgical repair of tetralogy of Fallot. N Engl J Med 1993;329:593–9.

20. Nollert G, Fischlein T, Bouterwek S, Bohmer C, Klinner W, Reichart B. Long-term survival in patients with repair of tetralogy of Fallot: 36-year follow-up of 490 survivors of the first year after surgical repair. J Am Coll Cardiol 1997;30:1374–83.

21. Saul JP, Alexander ME. Preventing sudden death after repair of tetralogy of Fallot: complex therapy for complex patients. J Cardiovasc Electrophysiol 1999;10:1271–87.

22. Kugler JD. Predicting sudden death in patients who have undergone tetralogy of Fallot repair: is it really as simple as measuring ECG intervals? J Cardiovasc Electrophysiol 1998;9:103–6.

23. Bricker JT. Sudden death and tetralogy of Fallot. Risks, markers, and causes. Circulation 1995;92:158–9.

24. Gatzoulis MA, Till JA, Somerville J, Redington AN. Mechanoelectrical interaction in tetralogy of Fallot. QRS prolongation relates to right ventricular size and predicts malignant ventricular arrhythmias and sudden death. Circulation 1995;92:231–7.

25. Berul CI, Hill SL, Geggel RL, Hijazi ZM, Marx GR, Rhodes J, Walsh KA, Fulton DR. Electrocardiographic markers of late sudden death risk in postoperative tetralogy of Fallot children. J Cardiovasc Electrophysiol 1997;8:1349–56.

26. Hokanson JS, Moller JH. Significance of early transient complete heart block as a predictor of sudden death late after operative correction of tetralogy of Fallot. Am J Cardiol 2001;87:1271–7.

27. Hamada H, Terai M, Jibiki T, Nakamura T, Gatzoulis MA, Niwa K. Influence of early repair of tetralogy of fallot without an outflow patch on late arrhythmias and sudden death: a 27-year follow-up study following a uniform surgical approach. Cardiol Young 2002;12:345–51.

28. Mackie AS, Gauvreau K, Perry SB, del Nido PJ, Geva T. Echocardiographic predictors of aortopulmonary collaterals in infants with tetralogy of fallot and pulmonary atresia. J Am Coll Cardiol 2003;41:852–7.

29. Geva T, Sahn, DJ, Powell AJ. Magnetic resonance imaging of congenital heart disease in adults. Progress in Pediatric Cardiology 2003;17:21–39.

30. Vick GW, 3rd, Wendt RE, 3rd, Rokey R. Comparison of gradient echo with spin echo magnetic resonance imaging and echocardiography in the evaluation of major aortopulmonary collateral arteries. Am Heart J 1994;127:1341–7.

31. Powell AJ, Chung T, Landzberg MJ, Geva T. Accuracy of MRI evaluation of pulmonary blood supply in patients with complex pulmonary stenosis or atresia. Int J Card Imaging 2000;16:169–74.

32. Holmqvist C, Hochbergs P, Bjorkhem G, Brockstedt S, Laurin S. Pre-operative evaluation with MR in tetralogy of fallot and pulmonary atresia with ventricular septal defect. Acta Radiol 2001;42:63–9.

33. Beekman RP, Beek FJ, Meijboom EJ. Usefulness of MRI for the pre-operative evaluation of the pulmonary arteries in Tetralogy of Fallot. Magn Reson Imaging 1997;15:1005–15.

34. Geva T, Greil GF, Marshall AC, Landzberg M, Powell AJ. Gadolinium-enhanced 3-dimensional magnetic resonance angiography of pulmonary blood supply in patients with complex pulmonary stenosis or atresia: comparison with x-ray angiography. Circulation 2002;106:473–8.

35. Helbing WA, de Roos A. Clinical applications of cardiac magnetic resonance imaging after repair of tetralogy of Fallot. Pediatr Cardiol 2000;21:70–9.

36. Geva T, Sandweiss BM, Gauvreau K, Lock JE, Powell AJ. Factors associated with impaired clinical status in long-term survivors of tetralogy of Fallot repair evaluated by magnetic resonance imaging. J Am Coll Cardiol 2004;43:1068–74.

37. Roest AA, Helbing WA, Kunz P, van den Aardweg JG, Lamb HJ, Vliegen HW, van der Wall EE, de Roos A. Exercise MR imaging in the assessment of pulmonary regurgitation and biventricular function in patients after tetralogy of fallot repair. Radiology 2002;223:204–11.

38. Rebergen SA, Chin JG, Ottenkamp J, van der Wall EE, de Roos A. Pulmonary regurgitation in the late postoperative follow-up of tetralogy of Fallot. Volumetric quantitation by nuclear magnetic resonance velocity mapping. Circulation 1993;88:2257–66.

39. Niezen RA, Helbing WA, van Der Wall EE, van Der Geest RJ, Vliegen HW, de Roos A. Left ventricular function in adults with mild pulmonary insufficiency late after Fallot repair. Heart 1999;82:697–703.

40. Niezen RA, Helbing WA, van der Wall EE, van der Geest RJ, Rebergen SA, de Roos A. Biventricular systolic function and mass studied with MR imaging in children with pulmonary regurgitation after repair for tetralogy of Fallot. Radiology 1996;201:135–40.

41. Davlouros PA, Kilner PJ, Hornung TS, Li W, Francis JM, Moon JC, Smith GC, Tat T, Pennell DJ, Gatzoulis MA. right ventricular function in adults with repaired tetralogy of Fallot assessed with cardiovascular magnetic resonance imaging: detrimental role of right ventricular outflow aneurysms or akinesia and adverse right-to-left ventricular interaction. J Am Coll Cardiol 2002;40:2044–52.

42. Prakash A, Powell AJ, Krishnamurthy R, Geva T. Magnetic resonance imaging evaluation of myocardial perfusion and viability in congenital and acquired pediatric heart disease. Am J Cardiol 2004;93:657–61.

43. Van Praagh R. The importance of segmental situs in the diagnosis of congenital heart disease. Semin Roentgenol 1985;20:254–71.

44. Blume ED, Altmann K, Mayer JE, Colan SD, Gauvreau K, Geva T. Evolution of risk factors influencing early mortality of the arterial switch operation. J Am Coll Cardiol 1999;33:1702–9.

45. Levinsky L, Srinivasan V, Alvarez-Diaz F, Subramanian S. Reconstruction of the new atrial septum in the Senning operation. New technique. J Thorac Cardiovasc Surg 1981;81:131–4.

46. Myridakis DJ, Ehlers KH, Engle MA. Late follow-up after venous switch operation (Mustard procedure) for simple and complex transposition of the great arteries. Am J Cardiol 1994;74:1030–6.

47. Redington AN, Rigby ML, Oldershaw P, Gibson DG, Shinebourne EA. Right ventricular function 10 years after the Mustard operation for transposition of the great arteries: analysis of size, shape, and wall motion. Br Heart J 1989;62:455–61.

48. Deanfield J, Camm J, Macartney F, Cartwright T, Douglas J, Drew J, de Leval M, Stark J. Arrhythmia and late mortality after Mustard and Senning operation for transposition of the great arteries. An eight-year prospective study. J Thorac Cardiovasc Surg 1988;96:569–76.

49. Van Praagh R, Jung WK. The arterial switch operation in transposition of the great arteries: anatomic indications and contraindications. Thorac Cardiovasc Surg 1991;39 Suppl 2:138–50.

50. Wernovsky G, Jonas RA, Colan SD, Sanders SP, Wessel DL, Castanneda AR, Mayer JE, Jr. Results of the arterial switch operation in patients with transposition of the great arteries and abnormalities of the mitral valve or left ventricular outflow tract. J Am Coll Cardiol 1990;16:1446–54.

51. Rehnstrom P, Gilljam T, Sudow G, Berggren H. Excellent survival and low complication rate in medium-term follow-up after arterial switch operation for complete transposition. Scand Cardiovasc J 2003;37:104–6.

52. Kramer HH, Scheewe J, Fischer G, Uebing A, Harding P, Schmiel F, Cremer J. Long term follow-up of left ventricular performance and size of the great arteries before and after one- and two-stage arterial switch operation of simple transposition. Eur J Cardiothorac Surg 2003;24:898–905.

53. Prifti E, Crucean A, Bonacchi M, Bernabei M, Murzi B, Luisi SV, Vanini V. Early and long term outcome of the arterial switch operation for transposition of the great arteries: predictors and functional evaluation. Eur J Cardiothorac Surg 2002;22:864–73.

54. Dunbar-Masterson C, Wypij D, Bellinger DC, Rappaport LA, Baker AL, Jonas RA, Newburger JW. General health status of children with D-transposition of the great arteries after the arterial switch operation. Circulation 2001;104:I138–42.

55. Losay J, Touchot A, Serraf A, Litvinova A, Lambert V, Piot JD, Lacour-Gayet F, Capderou A, Planche C. Late outcome after arterial switch operation for transposition of the great arteries. Circulation 2001;104:I121–6.

56. Mahle WT, McBride MG, Paridon SM. Exercise performance after the arterial switch operation for D-transposition of the great arteries. Am J Cardiol 2001;87:753–8.

57. Van Praagh R, Papagiannis J, Grunenfelder J, Bartram U, Martanovic P. Pathologic anatomy of corrected transposition of the great arteries: medical and surgical implications. Am Heart J 1998;135:772–85.

58. Beauchesne LM, Warnes CA, Connolly HM, Ammash NM, Tajik AJ, Danielson GK. Outcome of the unoperated adult who presents with congenitally corrected transposition of the great arteries. J Am Coll Cardiol 2002;40:285–90.

59. Colli AM, de Leval M, Somerville J. Anatomically corrected malposition of the great arteries: diagnostic difficulties and surgical repair of associated lesions. Am J Cardiol 1985;55:1367–72.

60. Van Praagh R. What is congenitally corrected transposition? N Engl J Med 1970;282:1097–8.

61. Chung KJ, Simpson IA, Glass RF, Sahn DJ, Hesselink JR. Cine magnetic resonance imaging after surgical repair in patients with transposition of the great arteries. Circulation 1988;77:104–9.

62. Lorenz CH, Walker ES, Graham TP, Jr., Powers TA. Right ventricular performance and mass by use of cine MRI late after atrial repair of transposition of the great arteries. Circulation 1995;92:II233–9.

63. Hardy CE, Helton GJ, Kondo C, Higgins SS, Young NJ, Higgins CB. Usefulness of magnetic resonance imaging for evaluating great-vessel anatomy after arterial switch operation for D-transposition of the great arteries. Am Heart J 1994;128:326–32.

64. Beek FJ, Beekman RP, Dillon EH, Mali WP, Meiners LC, Kramer PP, Meyboom EJ. MRI of the pulmonary artery after arterial switch operation for transposition of the great arteries. Pediatr Radiol 1993;23:335–40.

65. Theissen P, Kaemmerer H, Sechtem U, Luhmer I, Smolarz K, Kallfelz HC, Schicha H. Magnetic resonance imaging of cardiac function and morphology in patients with transposition of the great arteries following Mustard procedure. Thorac Cardiovasc Surg 1991;39(Suppl 3):221–4.

66. Rees S, Somerville J, Warnes C, Underwood R, Firmin D, Klipstein R, Longmore D. Comparison of magnetic resonance imaging with echocardiography and radionuclide angiography in assessing cardiac function and anatomy following Mustard's operation for transposition of the great arteries. Am J Cardiol 1988;61:1316–22.

67. Tulevski, II, Lee PL, Groenink M, van der Wall EE, Stoker J, Pieper PG, Romkes H, Hirsch A, Mulder BJ. Dobutamine-induced increase of right ventricular contractility without increased stroke volume in adolescent patients with transposition of the great arteries: evaluation with magnetic resonance imaging. Int J Card Imaging 2000;16:471–8.

68. Tulevski, II, van der Wall EE, Groenink M, Dodge-Khatami A, Hirsch A, Stoker J, Mulder BJ. Usefulness of magnetic resonance imaging dobutamine stress in asymptomatic and minimally symptomatic patients with decreased cardiac reserve from congenital heart disease (complete and corrected transposition of the great arteries and subpulmonic obstruction). Am J Cardiol 2002;89:1077–81.

69. Roest AA, Lamb HJ, van der Wall EE, Vliegen HW, van den Aardweg JG, Kunz P, de Roos A, Helbing WA. Cardiovascular response to physical exercise in adult patients after atrial correction for transposition of the great arteries assessed with magnetic resonance imaging. Heart 2004;90:678–84.

70. Videlefsky N, Parks WJ, Oshinski J, Hopkins KL, Sullivan KM, Pettigrew RI, Fyfe D. Magnetic resonance phase-shift velocity mapping in pediatric patients with pulmonary venous obstruction. J Am Coll Cardiol 2001;38:262–7.

71. Belli E, Serraf A, Lacour-Gayet F, Inamo J, Houyel L, Bruniaux J, Planche C. Surgical treatment of subaortic stenosis after biventricular repair of double-outlet right ventricle. J Thorac Cardiovasc Surg 1996;112:1570–8; discussion 1578–80.

72. Yoo SJ, Kim YM, Choe YH. Magnetic resonance imaging of complex congenital heart disease. Int J Card Imaging 1999;15:151–60.

73. Beekmana RP, Roest AA, Helbing WA, Hazekamp MG, Schoof PH, Bartelings MM, Sobotka MA, de Roos A, Ottenkamp J. Spin echo MRI in the evaluation of hearts with a double outlet right ventricle: usefulness and limitations. Magn Reson Imaging 2000;18:245–53.

74. Beekman RP, Beek FJ, Meijboom EJ, Wenink AC. MRI appearance of a double inlet and double outlet right ventricle with supero-inferior ventricular relationship. Magn Reson Imaging 1996;14:1107–12.

75. Igarashi H, Kuramatsu T, Shiraishi H, Yanagisawa M. Criss-cross heart evaluated by colour Doppler echocardiography and magnetic resonance imaging. Eur J Pediatr 1990;149:523–25.

76. Niezen RA, Beekman RP, Helbing WA, van der Wall EE, de Roos A. Double outlet right ventricle assessed with magnetic resonance imaging. Int J Card Imaging 1999;15:323–9.

77. Sorensen TS, Korperich H, Greil GF, Eichhorn J, Barth P, Meyer H, Pedersen EM, Beerbaum P. Operator-independent isotropic three-dimensional magnetic resonance imaging for morphology in congenital heart disease: a validation study. Circulation 2004;110:163–9.

78. Van Praagh R, Van Praagh S. The anatomy of common aorticopulmonary trunk (truncus arteriosus communis) and its embryologic implications. A study of 57 necropsy cases. Am J Cardiol 1965;16:406–25.

79. Collett RW, Edwards JE. Persistent truncus arteriosus: a classification according to anatomic types. Surg Clin North Am 1949;29:1245–70.

80. Litovsky SH, Ostfeld I, Bjornstad PG, Van Praagh R, Geva T. Truncus arteriosus with anomalous pulmonary venous connection. Am J Cardiol 1999;83:801–4, A810.

81. Goldmuntz E, Clark BJ, Mitchell LE, Jawad AF, Cuneo BF, Reed L, McDonald-McGinn D, Chien P, Feuer J, Zackai EH, Emanuel BS, Driscoll DA. Frequency of 22q11 deletions in patients with conotruncal defects. J Am Coll Cardiol 1998;32:492–8.

82. Tworetzky W, McElhinney DB, Brook MM, Reddy VM, Hanley FL, Silverman NH. Echocardiographic diagnosis alone for the complete repair of major congenital heart defects. J Am Coll Cardiol 1999;33:228–3.

83. Fyler DC, Buckley LP, Hellenbrand WE, Cohn HE. Report of the New England Regional Infant Cardiac Program. Pediatrics 1980;65:377–461.

84. Celoria GC, Patton RB. Congenital absence of the aortic arch. Am Heart J 1959;58:407–13.

85. Geva T, Gajarski RJ. Echocardiographic diagnosis of type B interruption of a right aortic arch. Am Heart J 1995;129:1042–5.

86. Kutsche LM, Van Mierop LH. Cervical origin of the right subclavian artery in aortic arch interruption: pathogenesis and significance. Am J Cardiol 1984;53:892–5.

87. Kaulitz R, Jonas RA, van der Velde ME. Echocardiographic assessment of interrupted aortic arch. Cardiol Young 1999;9:562–71.

88. Varghese A, Gatzoulis M, Mohiaddin RH. Images in cardiovascular medicine: Magnetic resonance angiography of a congenitally interrupted aortic arch. Circulation 2002;106:E9–10.

89. Tsai-Goodman B, Geva T, Odegard KC, Sena LM, Powell AJ. Clinical role, accuracy, and technical aspects of cardiovascular magnetic resonance imaging in infants. Am J Cardiol 2004;94:69–74.

90. Nielsen J, Powell AJ, Gauvreau K, Marcus E, Geva T. Magnetic resonance imaging predictors of the hemodynamic severity of aortic coarctation. J Am Coll Cardiol 2004;43:24A.